

INITIAL CHARACTERISTICS OF *KEPLER* SHORT CADENCE DATA

RONALD L. GILLILAND¹, JON M. JENKINS², WILLIAM J. BORUCKI³, STEVEN T. BRYSON³, DOUGLAS A. CALDWELL², BRUCE D. CLARKE², JESSIE L. DOTSON³, MICHAEL R. HAAS³, JENNIFER HALL⁴, TODD KLAUS⁴, DAVID KOCH³, SEAN MCCAULIFF⁴, ELISA V. QUINTANA², JOSEPH D. TWICKEN², AND JEFFREY E. VAN CLEVE²

Submitted to The Astrophysical Journal Letters

ABSTRACT

The *Kepler Mission* offers two options for observations – either Long Cadence (LC) used for the bulk of core mission science, or Short Cadence (SC) which is used for applications such as asteroseismology of solar-like stars and transit timing measurements of exoplanets where the 1-minute sampling is critical. We discuss the characteristics of SC data obtained in the 33.5-day long Quarter 1 (Q1) observations with *Kepler* which completed on 15 June 2009. The truly excellent time series precisions are nearly Poisson limited at 11th magnitude providing per-point measurement errors of 200 parts-per-million per minute. For extremely saturated stars near 7th magnitude precisions of 40 ppm are reached, while for background limited measurements at 17th magnitude precisions of 7 mmag are maintained. We note the presence of two additive artifacts, one that generates regularly spaced peaks in frequency, and one that involves additive offsets in the time domain inversely proportional to stellar brightness. The difference between LC and SC sampling is illustrated for transit observations of TrES-2.

Subject headings: planetary systems — stars: oscillations — techniques: photometric

1. INTRODUCTION

The *Kepler Mission* has a primary science goal of detecting analogs of the Earth orbiting stars in the extended solar neighborhood as reviewed in Borucki et al. (2009). Overall mission design and performance are reviewed by Koch et al. (2009). In this paper we establish the characteristics of data from *Kepler* collected at 1-minute cadence. Asteroseismology of solar-type stars requires detection of oscillations with periods of 3 – 10 minutes, which thus cannot be studied at the LC of nearly 30 minutes. Early science returns and goals of asteroseismology are reviewed by Gilliland et al. (2010). For exoplanets, precise determination of the transit times of many successive events to search for possible variations in those times due to the gravitational influence of other planets (Holman & Murray 2005) benefits from SC.

2. TARGET, DATA, AND CADENCE SPECIFICS

The *Kepler* targets in Q1 consisted of 156097 stars observed at LC. A mere 512 targets, or 0.3% of the total may be carried at the roughly one minute SC. A new SC target list may be used each month. Early in the mission nearly all the SC targets have been assigned to the *Kepler Asteroseismic Consortium* (KASC); some 4000 targets will be surveyed, each for one month from which the best set will be selected for extended observations. As planetary candidates are discovered many of these are switched to short cadence in order to provide precise transit timing variation (TTV) measures, and for accurate determinations of the host star mass and radius if

stellar oscillations can be detected. The asteroseismology program through KASC is guaranteed access to 140 SC target slots throughout the mission. At the start of Q2 (19 June 2009) 25 SC targets are reserved for the Guest Observer (GO) program.

There is also a restriction that the total number of pixels for SC not exceed $512 \times 85 = 43,520$. Very bright stars require more than 85 pixels each, thus requiring an SC target set with a balanced distribution of magnitudes.

Data is time-stamped so that the mid-time of each cadence is known with an accuracy of ± 0.050 seconds. Details of how the data acquisition process is managed on-board the spacecraft may be found in the “*Kepler Instrument Handbook*” (van Cleve & Caldwell 2009), as well as a wealth of general information that is beyond the scope of a *Letter*. Caldwell et al. (2009) discuss characteristics of the instrument and early calibration.

At the most basic level it is important to understand that the integrations underlying both SC and LC data are the same 6.02 s, followed by 0.52 s readout, before successive integrations are summed into memory. There is no difference at which saturation occurs for the 58.84876 s cadence data, versus the 29.4244 min LC, since both are based on 6 s exposures. Within the 58.85 s SC periods, 54.18 s is spent usefully collecting photons while the remainder of the time is divided between 9 readouts, which generates “smear” along the columns as *Kepler* has no shutter. This is removed (Jenkins et al. 2009a) as an early pipeline calibration step. In Q1 138 out of 49,170 cadences (<0.3%) were rejected, being associated with periods of excess spacecraft jitter yielding a 99.7% duty cycle (!) for these 33.49 days, which span HJD (-2454900) = 64.00 to 97.49.

LC data involve collection of collateral data continuously in a spatial sense along overscan (trailing black) columns, plus masked and virtual (smear) rows, while for SC only those collateral pixels that project onto the SC aperture are retained. Likewise, for LC there are 4464

gillil@stsci.edu

¹Space Telescope Science Institute, 3700 San Martin Drive, Baltimore, MD 21218

²SETI Institute/NASA Ames Research Center, MS 244-30, Moffett Field, CA 94035

³NASA Ames Research Center, MS 244-30, Moffett Field, CA 94035

⁴Orbital Sciences Corporation/NASA Ames Research Center, MS 244-30, Moffett Field, CA 94035

pixels on each channel assigned to apparently blank regions of the field to provide real time monitoring of sky brightness (which changes more than expected), SC does not have dedicated sky pixels, therefore interpolation between LC measures is used by the current pipeline processing. Sky was not expected to change on a time scale of minutes, and inclusion of direct background monitoring at SC would have increased telemetry needs for SC dramatically leading to an early decision to forgo this.

3. ERROR BUDGET, AND REALIZED NOISE LEVELS

In pre-launch simulations dozens of factors were considered in combination to arrive at predictions of noise levels in the *Kepler* data. In this *Letter* we consider the minimum number of error budget terms that together provide a good empirical representation of the realized noise level. With *Kepler's* exquisite precision most stars are variable at least on time scales of days. Detrending of photometric time series against variations of x, y pointing, thermal and focus changes is discussed by Jenkins et al. (2009b) for LC data. For SC applications where the time scales are usually short compared to thermal and focus forcing functions this is less of an issue, but still one that will remain a major analysis factor going forward.

The pipeline (Jenkins et al. 2009a) provides “raw” time series which are the simple sums (after cosmic ray and background removal) over the pixels chosen in an aperture to provide optimal signal-to-noise (S/N), the units of these are detected electrons (e-) per 58.8 s SC. To turn these time series into relative photometry with a mean of zero, and remove slow trends the following steps for each star have been taken: (1) A 5th order polynomial is fit to the full 33.5 days of data to remove drifts on timescales of a few days to a month resulting from minor pointing drift, focus changes etc. Future releases from the pipeline are expected to have more effective detrending, perhaps obviating any need for this step. (2) The polynomial fit is subtracted and then this value divided by the zero point term of the polynomial yielding zero mean, empirically detrended data. (3) A running median filter 361 cadences wide (6 hours) is evaluated and point-by-point subtracted from the data. SC data processed before November 2009 had an underlying software error that resulted in blocks of 3,000 successive pixels having photometric values too high by ~ 0.3 mmag at 12th magnitude (scaling inversely with brightness). These randomly positioned blocks averaged about one per star, are effectively suppressed in the current data by the median filter, and the software error has now been fixed in the pipeline. (4) The §4.1 correction is applied. (5) Any individual points more than $5\text{-}\sigma$ deviant from the mean of zero have values and weights set to zero. Typically this final step clips values for $<0.05\%$ of the data points.

Fig. 1 shows the result of forming power spectra for all 512 SC targets up to 8 mHz with a spacing of $0.05 \mu\text{Hz}$ that over-samples the frequency resolution by a factor of about seven, after transforming this to amplitude with an appropriate scale factor to have units of ppm. We then measure the noise level (standard deviation of the amplitude spectrum) over $\nu = 1 - 7.5$ mHz. Many stars have strong variations below 1 mHz, relatively fewer show significant power at higher frequencies, although a healthy subset of intrinsically variable stars show excess power at

high ν . (10 stars show high noise due to poorly designed apertures early in the mission.) Evident in Fig. 1 is a lower envelope of data points representing the empirical limit to precision as a function of magnitude.

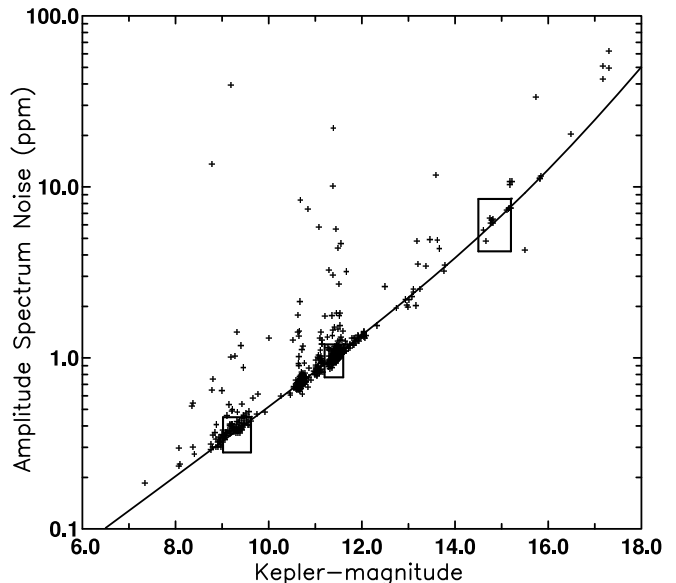


FIG. 1.— The noise level for each of 512 stars in Q1 Short Cadence data expressed as the standard deviation in ppm over 1.0 – 7.5 mHz in an amplitude spectrum (square root of power). The curve passing through the lower envelope consists of simple Poisson, readout noise plus sky background terms. The boxes near magnitudes of 9.3, 11.4 and 14.9 respectively are used to delineate samples of quiet stars as discussed in the text and Fig. 2. A minor spread in values is expected from differences in sensitivity and readout noise over the 84 amplifiers as well as errors in the *Kepler Input Catalog* magnitudes.

The Fig. 1 lower envelope is fit “by-eye” with $10^6(c + 9.5 \times 10^5(14.0/Kp)^5)^{1/2}/(cN^{1/2})$ where $c = 1.28 \times 10^{(0.4(12. - Kp) + 7)}$ is the number of detected e- per cadence and $N = 49032$ (the number of SCs used in Q1). In this empirical formulation aimed at achieving a minimal term model for the noise, c provides the Poisson term and is within the small channel-to-channel calibrated value for the count rate, Kp is the *Kepler* magnitude (close to R -band in center wavelength, but much broader, e.g. see Koch et al. 2009), and the $(14.0/Kp)^5$ term captures to first order the number of pixels used in the aperture extraction as a function of magnitude. We have assumed 8-pixel apertures at $Kp = 14$, increasing to 256 at $Kp = 7$. This in turn implies a per pixel variance of 11,875 per cadence, or a readout plus Poisson statistics on the sky of 109 e- per pixel per underlying 6 second exposure (9 per cadence). Since this is approximately the expected value (Caldwell et al. 2009) we conclude that this minimal model successfully represents the noise (as measured at high frequencies from amplitude spectra) in the data.

The set of 115 quiet stars at $Kp = 11.44$ has a mean time series rms of 255 ppm, and a mean amplitude noise level of 1.03 ppm. (The mean rms value divided by $N^{1/2}$ is 1.15 ppm, which is larger than the quoted amplitude spectrum noise level, since only the rms includes contributions from below 1 mHz.)

As a simple rule of thumb reaching a noise level of 1 ppm is required to make the most basic astero-

seismic measurement, that of determining the so-called large splitting $\Delta\nu_0$ which in turn can be used to accurately constrain the mean stellar density (see, e.g. Gilliland et al. 2010) in solar-type stars where several individual modes may be expected to have amplitudes of a few ppm. We reach this level with one month of data at $Kp \sim 11.3$. Coincidentally, $Kp \sim 11.3$ is also the rough dividing line below which stars saturate the detector during the 6 s integrations. It had long been a goal with *Kepler* to achieve photometry near the Poisson limit on strongly saturated stars as had been demonstrated for multiple *HST* CCD-based instruments without this having been a design goal (see, e.g. Gilliland (2004) for ACS). Nearly Poisson limited photometry is maintained to $Kp = 7$ (factor of 50 over-saturated), and beyond as long as the bleed does not extend into columns beyond the edge of the detector, nor blend with other bright stars. Photometry of highly saturated stars merely requires using an aperture that consistently captures the super-set of pixels that are bled into at any time over the time series. *The Kepler short cadence data have demonstrated a large dynamic range of 10 magnitudes, and for special applications can probably be extended usefully by one magnitude in each direction beyond the 7 – 17 range.*

A major factor contributing to the stability of *Kepler* photometry is the operating environment of the Earth-trailing orbit. The 2-axis, point-to-point jitter in SC centroids after removing a 5th order polynomial in x and y separately is 4.2×10^{-4} pixels, or only 1.7 milli-arcseconds. This remarkable result holds despite the use of two variable guide stars (removed for Q2) known to have degraded guiding in Q1 (Jenkins et al. 2009b).

4. KNOWN ANOMALIES IN CURRENT SC TIME SERIES

A number of anomalies, any specific one of which is a surprise, appear in the early *Kepler* SC data. The fact that some such unanticipated anomalies have arisen should not of course come as a surprise. We discuss the two most significant examples of these.

4.1. Power at 1/LC-period and Overtones

Fig. 2 illustrates the most serious artifact appearing in power spectra of SC time series. A number of peaks corresponding to the fundamental and all harmonics of the inverse of the LC-period, 29.4244 minutes, contaminate the spectra. Comparison of the amplitude of these modes shows that the effect is additive – as can be seen in Fig. 2 the relative amplitudes scale inversely with the stellar intensity. The causal factor may be variation in the detector electronics that “rings” in response to changes associated with initiation of each LC. For a given star these sinusoids appear to be coherent over the full 33 days, but different phases apply to each star. These peaks also appear in power spectra of the overscan (black) pixels. Attempts to ameliorate this effect, e.g. by using local sky variations from the periphery of SC target apertures, have failed to improve the situation. Further study will determine if changes to pipeline calibration can suppress this contamination which is introduced on the spacecraft. The SC photometry folded on the LC period (not shown) has significant ringing that is low amplitude near the boundaries, and larger peaks near the center at a time scale of 3 – 4 short cadences thus explaining the larger strength of intermediate harmonics,

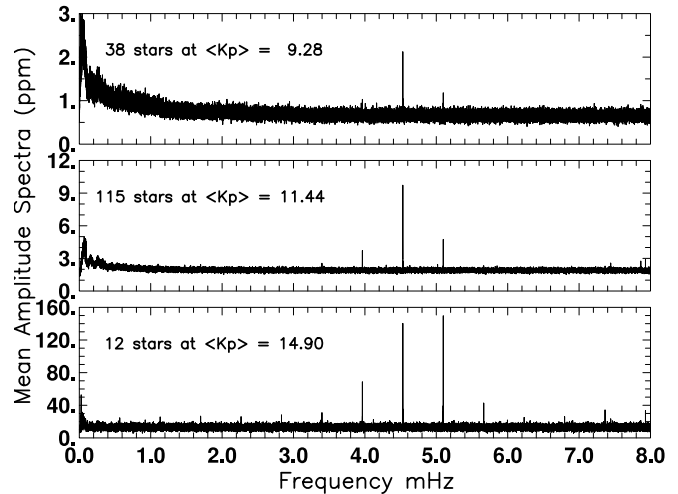


FIG. 2.— Mean amplitude spectra over samples of quiet stars spanning more than a factor of 100 in brightness are shown. The 1/LC-cadence artifacts at the fundamental of 0.566391 mHz and all harmonics are visible for the faint star set in the bottom panel. Even at 9th magnitude in the upper panel this artifact remains a dominant spectral feature from the 7th and 8th harmonics.

whether this robust empirical behavior is significant in understanding the origin remains under investigation.

For now, at least, asteroseismic investigations will either need to attempt corrections in the time or frequency domains on a star-by-star basis, or at a minimum flag frequencies at multiples of 0.566391 mHz as suspect. Since the fraction of “phase space” contaminated by these peaks is roughly the number of harmonics (14) times the frequency resolution (1/33-days), divided by 8 mHz, which equals 0.06%, the ultimate impact of these spurious peaks should be minimal.

With the exception of this artifact the *Kepler* spectra are remarkably clean and free of problematic sidelobes. The low frequency turn up in power for 9th magnitude stars below ~ 2 mHz in Fig. 2 likely follows from stellar oscillations and granulation noise which are easily seen in many individual amplitude spectra for bright stars. The peak at ~ 0.1 mHz likely corresponds to an artifact near 3.2 hours discussed in Jenkins et al. (2009b); the wavy structure at low frequency in the middle panel is likely due to harmonics of this.

4.2. Additive Corrections in the Time Domain

A somewhat more problematic artifact is illustrated in Fig. 3, but unlike that from the previous section, this can likely be addressed with pipeline modifications.

The primary offsets visible in Fig. 3 are vaguely transit-like, and clearly scale inversely with the intrinsic stellar intensity. These appear at the times of the two major brightening events seen in Q1 LC sky background (see §3 of Jenkins et al. 2009a for a discussion of these enigmatic and unexpected events) for which imperfect background correction is applied in the pipeline for these SC data. The correction illustrated adopts the mean from 115 stars near $Kp = 11.44$, and for points deviating by more than 8×10^{-5} from the mean of zero subtracts a scaled version of this. While not a perfect resolution, the primary features largely disappear, as well as several positive deviations appearing in the time series.

5. SCIENCE APPLICATIONS OF SC TIME SERIES

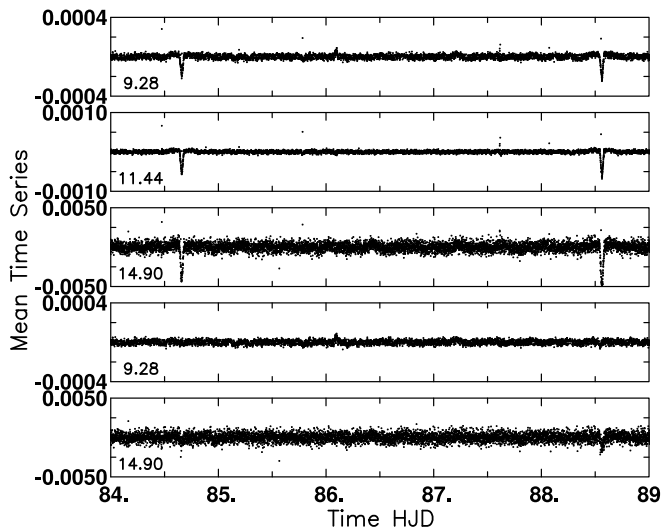


FIG. 3.— The upper three panels show means, after sigma clipping, over the same sets of stars shown in Fig. 2; this time however for 5 days of the direct time series. Events in the pipeline provided time series at HJD = 84.7 and 88.6 scale inversely with stellar brightness. The lower two panels show corrected mean time series for the 9th and 15th magnitude bins as discussed in the text.

5.1. Detailed Study of Transits

The previously known exoplanet hosts, TrES-2 (O’Donovan et al. 2006), HAT-P-7 (Pál 2008), and HAT-P-11 (Bakos et al. 2009) have all been observed at SC from the start. TrES-2b has the narrowest transits of these and is used to illustrate differences between LC and SC data in Fig. 4.

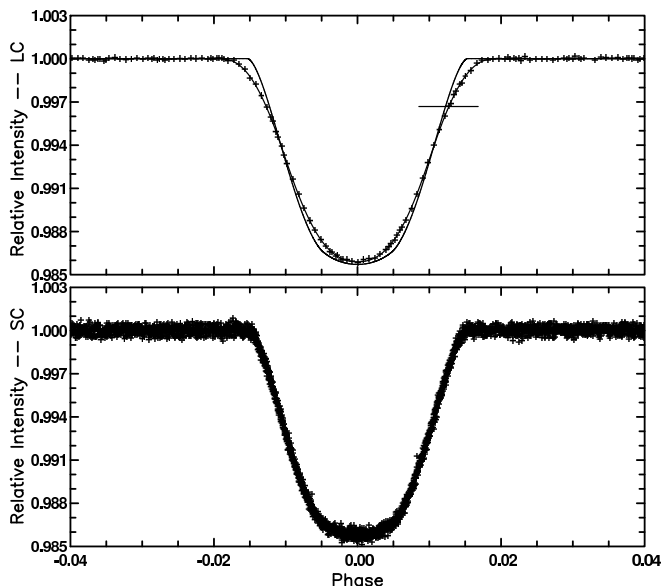


FIG. 4.— The upper panel shows the 33.5 days of Q1 LC data folded on the ~ 2.47 day period of TrES-2 with a *Kepler* magnitude of 11.34. The lower panel shows folded data at SC for the same interval. The curve passing through the points in the upper panel was based on fitting a transit light curve model *integrated* over the LC of 29.4 minutes, while for comparison the narrower curve (at top) shows the fit to SC data. The horizontal bar in the upper panel shows the length of an LC interval in phase for TrES-2.

LC observations effectively integrate over 29.4 minute intervals, which are not short compared to features in the TrES-2b transit, and therefore exhibit easily discerned

differences with respect to SC data which much more finely sample the light curve. The two fits shown in Fig. 4 use the Mandel & Agol (2002) transit model with identical values assumed for stellar mass, radius and limb-darkening. Parameters solved for are: $(R_p/R_*)^2$, the orbital period and phase, a zero point outside of transit, and a transit width related to the impact parameter. The SC model fit (*rms* residuals are 237 ppm) evaluates the functional representation at each central time, while the LC model fit (*rms* of 66 ppm) is integrated over the LC intervals (using a numerical sum corresponding to the 30 contributing SC intervals). Although the blurring introduced by the long LC intervals is very noticeable for TrES-2, the formal parameters returned from a simple non-linear, least-squares fit are nearly identical in the two cases. The solutions for planetary radius differ by only 0.012% for the LC and SC solutions, while the inferred orbital inclinations differ by only 0.001 degrees. Since systematic uncertainties on the stellar radius will likely remain $\gg 0.01\%$, even if asteroseismology solutions for the mean stellar density are available, LC data seem to equally well support determination of the basic parameters associated with transit modeling.

SC data are expected to provide a significant relative advantage for transit timings where LC data fail to resolve the critical ingress and egress periods. Quantification of this awaits applications to longer time series generally needed for TTV analyses.

5.2. Asteroseismology

The case for short cadence data for asteroseismic applications is clear. Indeed, the value of slightly less than 1-minute, rather than, say 2-minutes for SC data which would have been more convenient in terms of on-board data storage and telemetry bandwidth was selected to support robust asteroseismology of solar-like stars some of which will have modes with periods as short as 2 minutes. The Nyquist frequency for LC sampling of $283.2 \mu\text{Hz}$ permits asteroseismology on relatively large stars, e.g. the $R/R_\odot \sim 6$ star KOI-145 analyzed by Gilliland et al. (2010) has frequencies of maximum mode power (which scales with the surface acoustic cutoff frequency $\propto g/T_{eff}^{1/2}$ – Brown et al. 1991) at $143 \mu\text{Hz}$ and can be studied as effectively at LC as SC. Thus near solar temperatures, stars with radii down to R/R_\odot about 4 can be studied well at LC, for stars with radii below this SC data are needed.

6. DISCUSSION AND SUMMARY

We have shown that the 58.8 s short cadence data reaches *unparalleled* noise levels near fundamental limits imposed by Poisson statistics on source and background plus readout noise. An annoying artifact imposes frequencies at harmonics of the LC period in power spectra, but these are restricted to a few known frequencies and will not generally degrade science applications. SC data provide excellent returns in both transit and asteroseismic analyses. The SC data acquisition option is a limited resource that will be in great demand throughout the *Kepler* mission.

Funding for this Discovery Mission is provided by NASA’s Science Mission Directorate. We gratefully ac-

knowledge the many individuals through whose dedication and excellence the remarkable capabilities of *Kepler*

have been made possible.
Facilities: The Kepler Mission.

REFERENCES

- Bakos, G.Á., et al. 2009, ApJ, submitted, arXiv:0901.0282
Borucki, W.J., et al. 2009, Science, submitted
Brown, T.M., Gilliland, R.L., Noyes, R.W., & Ramsey, L.W. 1991, ApJ, 368, 599
Caldwell, D., et al. 2009, ApJ, submitted
Gilliland, R.L. 2004, INS ACS 2004-01, (STScI)
Gilliland, R.L., et al. 2010, PASP, in press.
Holman, M.J., & Murray, N.M. 2005, Science, 307, 1288
Jenkins, J.M., et al. 2009a, ApJ, submitted.
Jenkins, J.M., et al. 2009b, ApJ, submitted.
Koch, D., et al. 2009, ApJ, submitted.
Mandel, K., & Agol, E. 2002, ApJ, 580, L171
O'Donovan, F.T., et al. 2006, ApJ, 651, L61
Pál, A., et al. 2008, ApJ, 680, 1450
van Cleve, J., & Caldwell, D. 2009, *Kepler Instrument Handbook* (KSCI-19033), Version 1 (NASA-Ames)